ORIGINAL PAPER

The dynamic behavior of spiral waves in stochastic Hodgkin–Huxley neuronal networks with ion channel blocks

Shao-Bao Liu · Ying Wu · Jia-Jia Li · Yong Xie · Ning Tan

Abstract Chemical blocking is known to affect neural network activity. Here, we quantitatively investigate the dynamic behavior of spiral waves in stochastic Hodgkin–Huxley neuronal networks during sodium- or potassium-ion channel blockages. When the sodium-ion channels are blocked, the spiral waves first become sparse and then break. The critical factor for the transition of spiral waves (x_{Na}) is sensitive to the channel noise. However, with the potassium-ion channel block, the spiral waves first become intensive and then form other dynamic patterns. The critical factor for the transition of spiral waves (x_K) is insensitive to the channel noise. With the sodium-ion channel block, the spike frequency of a single neuron in the network is reduced, and the collective excitability of the neuronal network weakens. By blocking the potassium ion channels, the spike frequency of a single neuron in the network increases, and the collective excitability of the neuronal network is enhanced. Lastly, we found that the behavior of spiral waves is directly related to the system synchronization. This research will enhance our un-

derstanding of the evolution of spiral waves through toxins or drugs and will be helpful to find potential applications for controlling spiral waves in real neural systems.

1 Introduction

Neural-information processing results from collaboration and interaction between dozens of diverse ion channels. Experimental studies show that some toxins can change the properties of neuronal ion channels; for example, tetraethylammonium (TEA) and tetrodotoxin (TTX) can block potassium- and sodium-ion channels, respectively. These blockages, in turn, reduce the number of working channels. As a result, the effective conductance of a membrane patch decreases, and the noise effect of ion channels is enhanced. Thus, the block of a single ion channel can potentially affect the collective spiking activities of an entire neural network. Understanding the acute effects of these blockages is thus vital for enhancing our understanding of how entire neural systems may be modified in response to such blockages.

The development of the Hodgkin–Huxley (H–H) model [1], which describes the action potential of a membrane patch of a neuron, allowed the mathematical study of a number of neural-related phenom-

S.-B. Liu · Y. Wu (✉) · J.-J. Li · Y. Xie · N. Tan
State Key Laboratory for Strength and Vibration of
Mechanical Structures, School of Aerospace, Xi'an
Jiaotong University, Xi'an 710049, China
e-mail: wying36@163.com

S.-B. Liu
Department of Engineering Mechanics, School of Civil
Engineering and Architecture, Xi'an University of
Technology, Xi'an 710048, China

ena [2–6]. For example, Schmid et al. [5, 6] investigated the effects of a channel block on the spiking activity of excitable membranes using an H–H model with stochastic, ion-channel gating. They showed that it is possible to increase or decrease the regularity of spontaneous spike trains by blocking some portion of potassium- or sodium-ion channels. Gong et al. [7] studied the effects of a channel block on the collective spiking activity of an array of bidirectionally coupled stochastic H–H neurons. Their results reveal that the effects of sodium- or potassium-ion channel blocks on the collective spiking activity of coupled neurons are different from their effects on the spiking activity of a single neuron. Mahmut Ozer et al. [8] investigated the regularity of spontaneous-spiking activity based on Newman–Watts' small-world neuronal networks, with a fraction of blocked, sodium-, and potassium-ion channels. It is shown that the coherence resonance-like phenomenon depends significantly and can be controlled via the fraction of closed sodium and potassium ion channels.

Spatiotemporal patterns are ubiquitous in biological systems and are observed in diverse systems as epidemiology [9], predator–prey systems [10], and pathogen dispersal [11]. Spiral waves are a class of spatiotemporal patterns that exist in cardiac tissue [12, 13] and the neocortex [14]. However, modern medicine has shown that spiral waves in heart tissue are not beneficial to human health. Instead, they are related to ventricular tachycardia (VT), which may cause ventricular fibrillation (VF) [12, 15, 16]. Fortunately, spiral waves are periodic and controllable. Therefore, much effort has been made to understand how to control such waves [17–19]. Wang et al. [20] confirmed that spiral waves can be effectively controlled in networks composed of Chua Circuits by using a certain kind of intermittent scheme. More recently, experimental [12] and numerical [21] studies have shown that spiral waves can be controlled through the use of toxins or drugs, such as beryllium, TTX, and TEA. However, most of these studies are observational, and the direct effects of toxins or drugs on the control of spiral waves are not well understood.

In this paper, we examine the influence of sodium- and potassium-ion channel blocks on the development of spiral waves in a stochastic two-dimensional H–H neuronal network model. To quantify our observations, we introduce the wave length (WL) measure of the spiral wave and the mean action potential duration

(MAPD) measure of a single neuron. The wave length (WL) is measured by calculating the mean number of silent neurons between two successive spiking parts in a row of neurons in the network. This quantity thus describes the sparseness of the spiral wave. In addition, the firing possibility and synchronization factor are both introduced to analyze the collective excitability of neurons and the mechanism of their synchronization.

2 Model of the stochastic H–H neuronal network with an ion-channel block

The dynamics of a two-dimensional H–H neuronal network with nearest-neighbor couplings in the presence of channel noise is given by [21]:

$$
\begin{aligned}
C_m \frac{dV_{ij}}{dt} = &-G_{\text{Na}}(m_{ij}, h_{ij})(V_{ij} - V_{\text{Na}}) \\
&- G_{\text{K}}(n_{ij})(V_{ij} - V_{\text{K}}) - G_L(V_{ij} - V_L) \\
&+ I_{\text{ext}} + D(V_{i-1j} + V_{i+1j} \\
&+ V_{ij-1} + V_{ij+1} - 4V_{ij}),
\end{aligned} \tag{1}
$$

where I_{ext} is the external stimulus, D is the coupling intensity, which holds the same physical unit as conductance, and the variables m, h, and n describe the mean ratios for the open gates of the three different working channels, respectively. In the presence of channel noise, the gate variables become stochastic quantities obeying the following Langevin equations [22]:

$$
\begin{aligned}
\frac{dy_{ij}}{dt} &= \alpha_y(V_{ij})(1 - y_{ij}) - \beta_y(V_{ij})y_{ij} + \xi_y(t), \\
&(y = m, h, n),
\end{aligned} \tag{2}
$$

where the voltage-dependent opening and closing rates $\alpha_y(V)$ and $\beta_y(V)$ are described as follows [23, 24]:

$$
\begin{aligned}
\alpha_m &= 0.1(V_{ij} + 40)/\big(1 - \exp\big(-(V_{ij} + 40)/10\big)\big), \\
\alpha_h &= 0.07 \exp\big((-V_{ij} + 65)/20\big), \\
\alpha_n &= 0.01(V_{ij} + 55)/\big(1 - \exp\big(-(V_{ij} + 55)/10\big)\big), \\
\beta_m &= 4 \exp\big(-(V_{ij} + 65)/18\big), \\
\beta_h &= 1/\big(1 + \exp\big(-(V_{ij} + 35)\big)/10\big), \\
\beta_n &= 0.125 \exp\big(-(V_{ij} + 65)/80\big).
\end{aligned} \tag{3}
$$

The sodium and potassium conductance with blocked ion channels are described by [5, 8]

$$
\begin{aligned}
G_{\mathrm{Na}}(m_{ij}, h_{ij}) &= g_{\mathrm{Na}}^{\max} x_{\mathrm{Na}} m_{ij}^3 h_{ij}, \\
G_{\mathrm{K}}(n_{ij}) &= g_{\mathrm{K}}^{\max} x_{\mathrm{K}} n_{ij}^4,
\end{aligned}
\tag{4}
$$

where the factors x_{K} and x_{Na} ($0 < x_{\mathrm{Na}}, x_{\mathrm{K}} < 1$) are the fraction of working channels (nonblocked) to the overall number of potassium-ion channels N_{K} and sodium-ion channels N_{Na}, respectively. A higher value of x_{Na} or x_{K} represents a lower degree of channel blockage (i.e., a large number of active ion channels). The variables g_{Na} and g_{K} denote the maximal conductance of sodium and potassium when all ion channels are open. In the numerical simulation, $g_{\mathrm{Na}}^{\max} = 120 \text{ mS/cm}^2$ and $g_{\mathrm{K}}^{\max} = 36 \text{ mS/cm}^2$. The variable $\xi_y(t)$ ($y = m, h, n$) is a Gaussian white noise with a mean value of zero. For an excitable membrane patch with N_{Na} sodium and N_{K} potassium ion channels, the noise correlations are described by [1, 7]

$$
\begin{aligned}
\langle \xi_m(t)\xi_m(t') \rangle &= \frac{2\alpha_m \beta_m}{N_{\mathrm{Na}} x_{\mathrm{Na}}(\alpha_m + \beta_m)} \delta(t - t'), \\
\langle \xi_h(t)\xi_h(t') \rangle &= \frac{2\alpha_h \beta_h}{N_{\mathrm{Na}} x_{\mathrm{Na}}(\alpha_h + \beta_h)} \delta(t - t'), \\
\langle \xi_n(t)\xi_n(t') \rangle &= \frac{2\alpha_n \beta_n}{N_{\mathrm{K}} x_{\mathrm{K}}(\alpha_n + \beta_n)} \delta(t - t').
\end{aligned}
\tag{5}
$$

The numbers of ion channels are $N_{\mathrm{Na}} = \rho_{\mathrm{Na}} S$ and $N_{\mathrm{K}} = \rho_{\mathrm{K}} S$, where S is the excitable membrane patch size. The level of noise increases as S decreases. Thus, S reflects the strength of the channel noise.

In our numerical simulations, homogeneous ion channel densities are given as $\rho_{\mathrm{Na}} = 60 \ \mu\mathrm{m}^{-2}$ and $\rho_{\mathrm{K}} = 18 \ \mu\mathrm{m}^{-2}$, and the capacitance of the membrane is $C_m = 1 \ \mu\mathrm{F/cm}^2$. The variables $V_{\mathrm{Na}} = 50 \text{ mV}$ and $V_{\mathrm{K}} = -77 \text{ mV}$ are the reversal potentials for sodium and potassium, respectively. The leakage potential is $V_L = -54.4 \text{ mV}$ [1], and the leakage conductance is $G_L = 0.3 \text{ mS/cm}^2$.

3 Simulation results and discussion

We simulated spatiotemporal patterns in a 100×100 neuronal network using the Euler method, with a time step of 0.02 units, and the no-flux boundary condition. The stimulating current was $I_{\mathrm{ext}} = 6.1 \ \mu\mathrm{A}$, and the coupling intensity was $D = 0.5 \text{ mS/cm}^2$. The initial conditions were given as: $V_{ij} = -40.2$, $m_{ij} = 0.1203$, $h_{ij} = 0.9$, $n_{ij} = 0.9$ ($i = 41 : 43$ & $j = 1 : 50$);

$V_{ij} = 0$, $m_{ij} = 0.5203$, $h_{ij} = 0.7$, $n_{ij} = 0.7$ ($i = 44 : 46$, $j = 1 : 50$); $V_{ij} = 40.0$, $m_{ij} = 0.98203$, $h_{ij} = 0.5$, $n_{ij} = 0.5$ ($i = 47 : 49$, $j = 1 : 50$); $V_{ij} = -61.19389$, $m_{ij} = 0.08203$, $h_{ij} = 0.46012$, $n_{ij} = 0.37726$ (rest sites). These initial values produce a stable spiral wave in neuronal networks. This pattern was confirmed by testing larger networks, which demonstrated that the behavior of spiral waves is unaffected by network size, as has been previously reported [21].
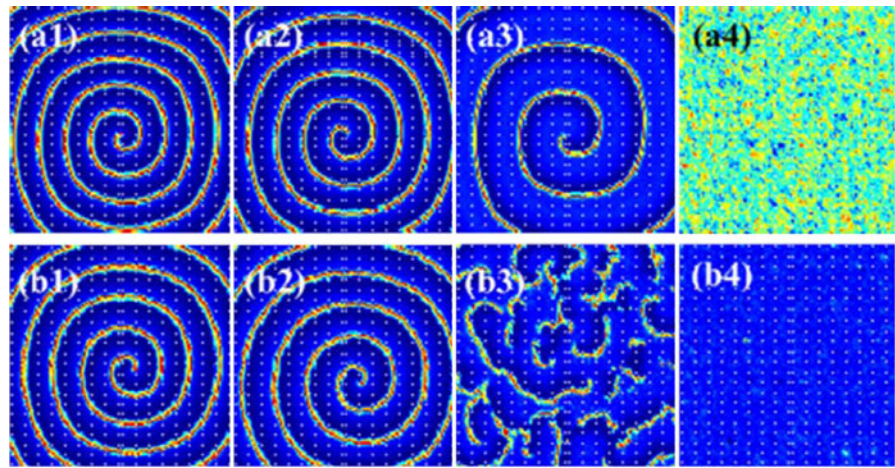
3.1 Sodium-ion channel block

We will first consider the channel block of a sodium ion. Figure 1a shows the spiral waves in networks of neurons with membrane patch sizes of 200 μm² and 5 μm², and sodium-ion channel block factors (x_{Na}) of 1.00, 0.75, 0.50, and 0.25. Stable spiral waves in a nonblock neuronal network ($x_{\mathrm{Na}} = 1$) are shown in Fig. 1a (a1, b1). As the degree of ion-channel block increased (e.g., when the factor x_{Na} decreases), the spiral waves broke up and their fragments filled up the network of neurons with smaller membrane patch sizes ($S = 5 \ \mu\mathrm{m}^2$). This is represented in Fig. 1a (see b3 and b4). However, as the size of the membrane patch increased ($S = 200 \ \mu\mathrm{m}^2$), the spiral waves became more sparse and then broke and became uniform (Fig. 1a; see a3 and a4). In short, the transition of spiral waves is induced by the blockage of sodium-ion channels, and this transition occurs more rapidly if strong channel noise is imposed on the networks. Similar results can be found by examining the spiking activities of a single neuron at the site (9, 10) in network. The spike train intervals are changed from regular to irregular, also from intensive to sparse, as seen in Fig. 1b.

In order to quantitatively describe the evolution of spiral waves, Fig. 2a shows the curves of the WL of spiral waves versus different block factor (x_{Na}) values at 500 time units for smaller and larger membrane patch sizes. WL becomes longer as the x_{Na} becomes smaller. The trends are consistent for different membrane patch sizes. Figure 2b shows the MAPD of a single neuron within 500 time units. The curves of MAPD increase as x_{Na} decreases for both small and large membrane patch sizes. This finding is consistent with results examining the spiking activity of single neurons [5, 6].
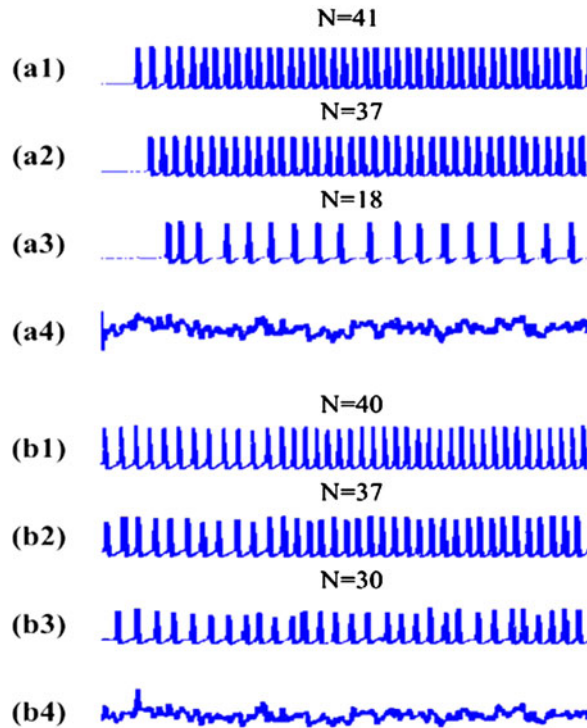
3.2 Potassium-ion channel block

We next examined the effects of potassium-ion channel blocks on spatiotemporal patterns. Figure 3a shows

(a)

(b)

the spiral waves in neuronal networks with membrane patch sizes of 200 μm² and 5 μm², and with potassium-ion channel block factors of 1.00, 0.75, 0.50, and 0.25. Initially, a stable spiral wave occurred in the nonblock neuronal network ($x_K = 1$), as shown in Fig. 3a (see a1 and b1). As x_K decreased, the spiral waves became more intense for both small ($S =$ 5 μm²) and large ($S = 200\ \mu m^2$) membrane patch sizes (Fig. 3a; see a2, a3, b2, and b3). However, when x_K became small ($x_K = 0.25$), different spatiotemporal patterns were induced for small and large membrane patch sizes (Fig. 3a; see a4 and b4). The spike train of the action potential of a single neuron at the site (9, 10) in the network is shown in Fig. 3b. The
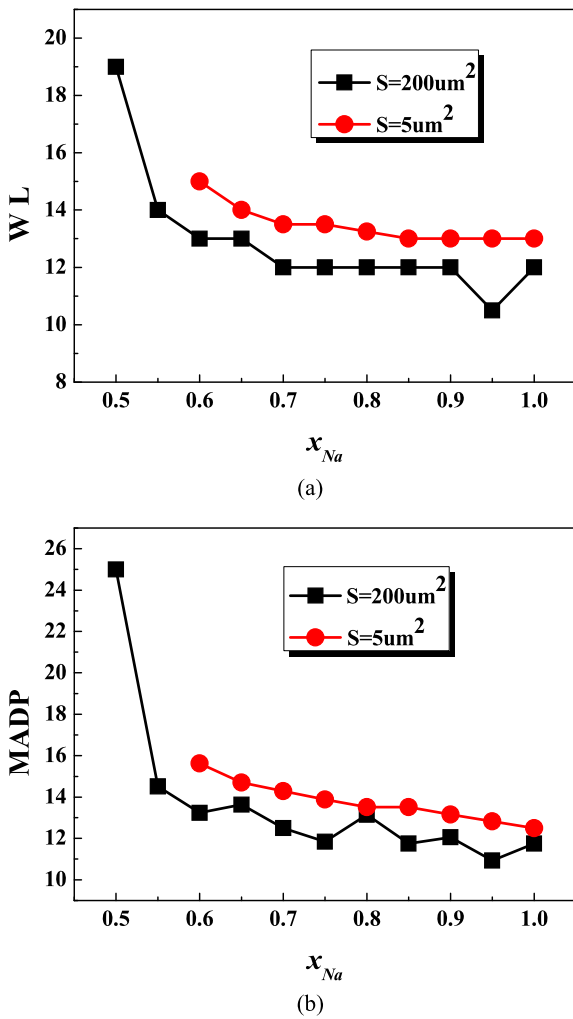
Fig. 2 (**a**) The wave length (WL) of a spiral wave at 500 time units and (**b**) the mean action potential duration (MAPD) of a single neuron within 500 time units. Sodium-ion channel block factors vary

spike train becomes more regular and intense as x_K decreases, which is different from our previous results with sodium-ion channel blocks (see above).

The WL of spiral waves and the MAPD of a single neuron at site (9, 10) in the network are presented in Fig. 4. For both large and small patch sizes, WL became small as x_K decreased. The MAPD values are similar: MAPD decreased slightly as x_K decreased, for both large and small membrane patch sizes. These results are in agreement with previous studies by Schmid et al. [5, 6].

In summary, the WL of spiral waves describes the macroscopic properties of the network, while MAPD

values illustrate the microscopic performance of a single neuron. Our studies found that WL and MAPD were generally consistent. The WL/MAPD ratio is almost a constant, which means that the conduction velocity ($\sim$WL/MAPD) of a spiral wave is unchangeable, regardless of patch size. As we know that the conduction velocity of a spiral wave is dependent on the coupling intensity, which is proportional to the square root of the coupling intensity. In our work the coupling intensity D is a constant, and thus our results are reasonable and reliable.

3.3 Statistical analyses

In order to understand the mechanism of the evolution of spiral waves in a stochastic neuronal network with an ion-channel block, we introduced both the firing possibility and the synchronization factor, which characterize the collective behavior and regularity of neuronal spikes. The firing possibility at $t = k$ is given by

$$P(k) = \frac{m}{N^2}, \tag{6}$$

where m is the number of firing neurons, which is defined as the neuronal membrane potential $V_{i,j} > -55$ mV at $t = k$ time units, and N^2 represents the total number of neurons in the network.

Based on the mean-field theory, the synchronization factor in the two-dimensional array can be defined as follows [19, 21]:

$$R = \frac{\langle F^2 \rangle - \langle F \rangle^2}{\frac{1}{N^2} \sum_{i=1}^{N} \sum_{j=1}^{N} (\langle V_{ij}^2 \rangle - \langle V_{ij} \rangle^2)}, \tag{7}$$

where F is the mean membrane potential of neurons in the network. F can be described as

$$F = \frac{1}{N^2} \sum_{i=1}^{N} \sum_{j=1}^{N} V_{ij}. \tag{8}$$

The firing possibilities of neurons in the network with the sodium-ion channel block are shown in Fig. 5a. As x_{Na} decreases, the firing likelihood decreases for both large and small membrane patch sizes. Furthermore, the neurons in the network barely fire ($p \approx 0$) when x_{Na} reaches a smaller value ($x_{Na} < 0.4$). This suggests that the sodium-ion channel block diminishes the collective excitability of neurons in the networks.

Fig. 3 (**a**) Spiral waves in H–H neuronal networks for membrane patch sizes of $S = 200\ \mu m^2$ (a1–a4) and $S = 5\ \mu m^2$ (b1–b4), at $t = 500$ time units. Potassium-ion block factors are 1.00 (a1, b1), 0.75 (a2, b2), 0.50 (a3, b3), and 0.25 (a4, b4). (**b**) Action potential of a single neuron at site (9, 10), for $S = 200\ \mu m^2$ (a1–a4), and $S = 5\ \mu m^2$ (b1–b4). Potassium-ion block factors are 1.00 (a1, b1), 0.75 (a2, b2), 0.50 (a3, b3), and 0.25 (a4, b4)
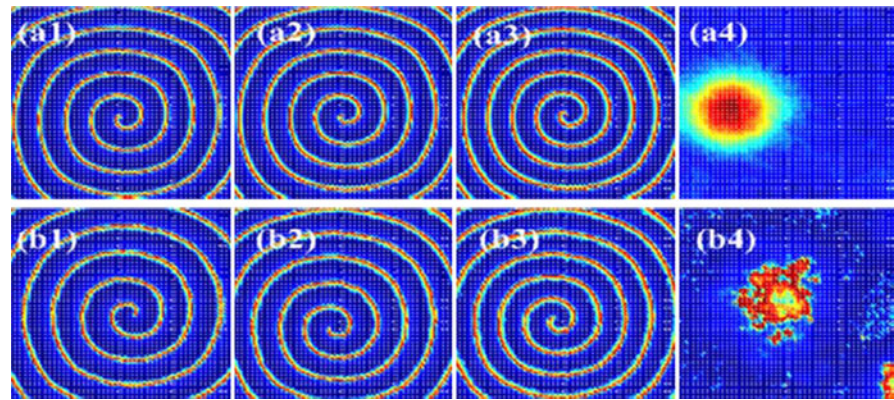

(a)
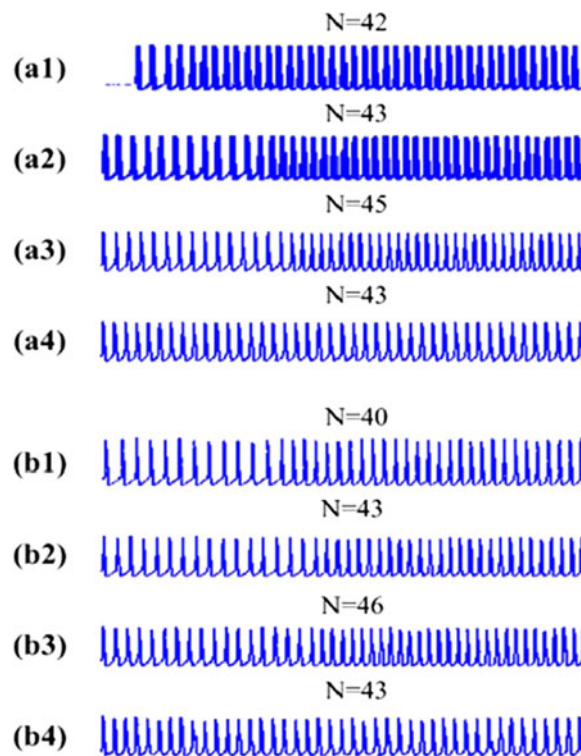
(b)

Additionally, the firing likelihood of neurons in the network with potassium-ion channel blocks is plotted in Fig. 5b. As the degree of potassium-ion channel block deepens, the firing likelihood increases when $x_K > 0.25$, which is the opposite of what occurs with sodium-ion channel blocks. This suggests that the collective excitability of neurons is enhanced by blocking potassium-ion channels.

Figure 6a shows the synchronization factor of the system with a sodium-ion channel block with 500 time units. The same turning point ($x_{Na} \approx 0.45$) on the two curves of synchronization factors was recovered for both large and small membrane patch sizes, even though they showed different outcomes. The turning point of the synchronization factors corresponds to x_{Na} for the transition of spiral waves, which is shown in

(a)

(b)
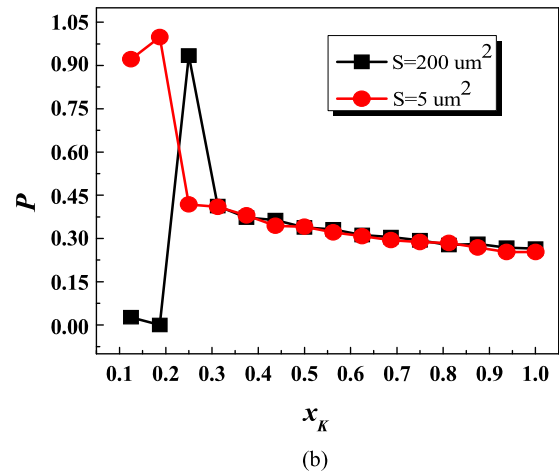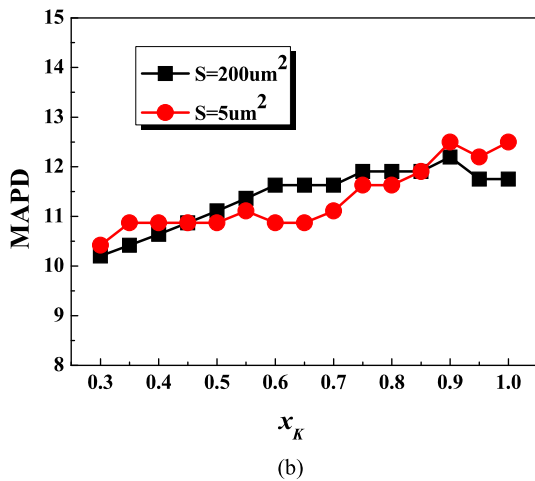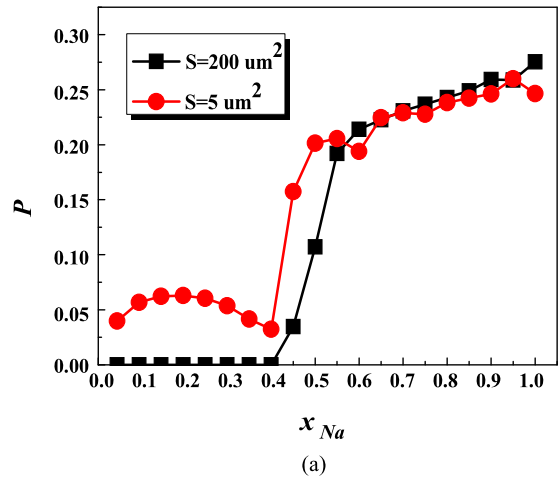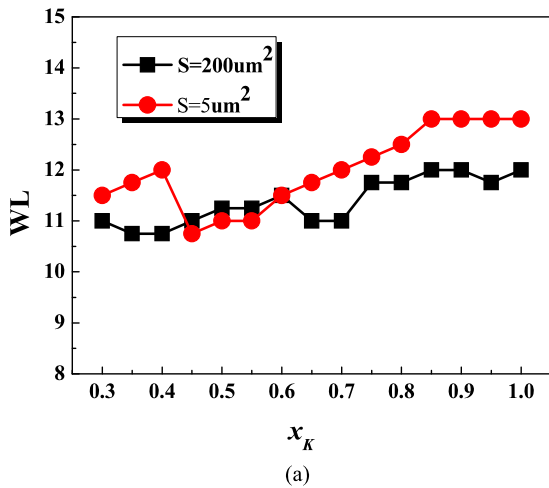
Fig. 4 (**a**) The wave length (WL) of a spiral wave at 500 time units. (**b**) The mean action potential duration (MAPD) of a single neuron within 500 time units. Potassium-ion channel block values vary


(a)

(b)

Fig. 5 Firing likelihood ($k = 500$ time units) vs. the block factors (**a**) sodium-ion channel block and (**b**) potassium-ion channel block

Fig. 1a (a3 → a4, b3 → b4). Figure 6b illustrates the synchronization factors of the system with the potassium-ion channel block. The two curves hold the same turning point ($x_K \approx 0.3$) for both large and small membrane patch sizes. At the same time, the transition of the spiral waves occurs near the turning point of the synchronization factor, as seen in Fig. 1b (a3 → a4, b3 → b4).

4 Conclusion

We investigated the effects of sodium- and potassium-ion channel blocks on the evolution of spatiotemporal patterns in stochastic Hodgkin–Huxley neuronal networks. We examined the transitional behaviors of spiral waves with the different degrees of sodium- and potassium-ion channel blocks. Our results showed that when sodium-ion channel blocks are imposed, the spiral waves first become sparse and then break. The transition occurs more rapidly if a stronger channel noise is imposed on the networks with the sodium-ion channel block. The critical factor x_{Na} is sensitive to channel noise. In contrast, we found that when we blocked potassium-ion channels, the spiral waves became intense and then formed different dynamic patterns. The critical factor x_K was unaffected by the channel noise. Furthermore, statistical analyses showed that the spike frequency of a single neuron is reduced and that the collective excitability of the whole neuronal network
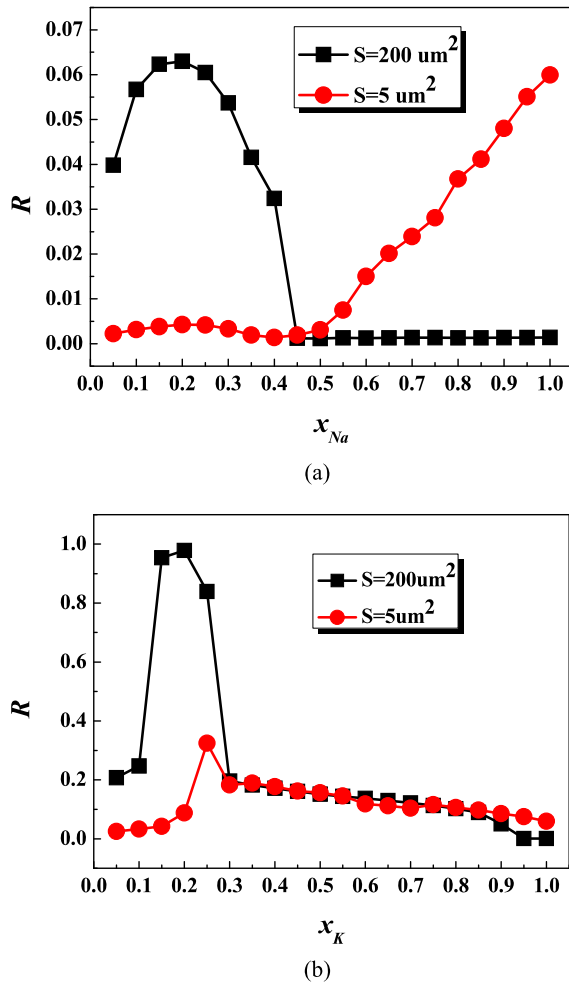
Fig. 6 Synchronization factor versus the block factors (within 500 time units) (**a**) sodium-ion channel block and (**b**) potassium-ion channel block

is weakened by the blockage of sodium-ion channels. In contrast, only the collective excitability of neuronal network is enhanced by the blockage of potassium-ion channels. The congruence we recovered between the turning points of synchronization factors and the transition of spiral waves demonstrates that the evolution of spiral waves is related to the synchronization of the system as a whole. Our findings provide new insight into controlling the evolution of spiral waves through the use of toxins or drugs. Thus, our study is an important first step in examining the potential application of drug/toxin blocks for controlling spiral waves in real neural systems.

References

1. Hodgkin, A.L., Huxley, A.F.: A quantitative description of membrane current and its application to conduction and excitation in nerve. J. Physiol. **117**, 500–544 (1952)
2. Yu, Y., Shu, Y., McCormick, D.A.: Cortical action potential backpropagation explains spike threshold variability and rapid-onset kinetics. J. Neurosci. **28**(29), 7260–7272 (2008)
3. Sun, X., Perc, M., Lu, Q., Kurths, J.: Spatial coherence resonance on diffusive and small-world networks of Hodgkin–Huxley neurons. Chaos **18**, 023102 (2008)
4. Lin, M., Luo, Z.Y., Bai, B.F., Xu, F., Lu, T.J.: Fluid mechanics in dentinal microtubules provides mechanistic insights into the difference between hot and cold dental pain. PLoS ONE **6**, e18068 (2011)
5. Schmid, G., Goychuk, I., Hänggi, P.: Effect of channel block on the spiking activity of excitable membranes in a stochastic Hodgkin–Huxley model. Phys. Biol. **1**, 61 (2004)
6. Schmid, G., Goychuk, I., Hänggi, P.: Controlling the spiking activity in excitable membranes via poisoning. Physica A **344**, 665–670 (2004)
7. Gong, Y.B., Xu, B., Ma, X.G., Han, J.Q.: Effect of channel block on the collective spiking activity of coupled stochastic Hodgkin–Huxley neurons. Sci. China Ser. B **51**, 341–346 (2008)
8. Ozer, M., Perc, M., Uzuntarla, M.: Controlling the spontaneous spiking regularity via channel blocking on Newman–Watts networks of Hodgkin–Huxley neurons. Europhys. Lett. **86**, 40008 (2009)
9. Sun, G.Q.: Pattern formation of an epidemic model with diffusion. Nonlinear Dyn. **69**, 1097–1104 (2012)
10. Sun, G.Q., Jin, Z., Li, L., Li, B.L.: Self-organized wave pattern in a predator–prey model. Nonlinear Dyn. **60**, 265–275 (2010)
11. Vasiev, B., Siegert, F., Weijer, C.: Multiarmed spirals in excitable media. Phys. Rev. Lett. **78**, 2489–2492 (1997)
12. Garfinkel, A., Kim, Y.H., Voroshilovsky, O., Qu, Z., Kil, J.R., Lee, M.H., Karagueuzian, H.S., Weiss, J.N., Chen, P.S.: Preventing ventricular fibrillation by flattening cardiac restitution. Proc. Natl. Acad. Sci. USA **97**, 6061 (2000)
13. Bursac, N., Aguel, F., Tung, L.: Multiarm spirals in a two-dimensional cardiac substrate. Proc. Natl. Acad. Sci. USA **101**, 15530 (2004)
14. Huang, X., Troy, W.C., Yang, Q., Ma, H., Laing, C.R., Schiff, S.J., Wu, J.Y.: Spiral waves in disinhibited mammalian neocortex. J. Neurosci. **24**, 9897 (2004)
15. Davidenko, J.M., Pertsov, A.V., Salomonsz, R., Baxter, W., Jalife, J.: Stationary and drifting spiral waves of excitation in isolated cardiac muscle. Nature **355**, 349–351 (1992)
16. Jalife, J.: Ventricular fibrillation: mechanisms of initiation and maintenance. Annu. Rev. Physiol. **62**, 25–50 (2000)
17. Hu, G., Xiao, J., Chua, L.O., Pivka, L.: Controlling spiral waves in a model of two-dimensional arrays of Chua's circuits. Phys. Rev. Lett. **80**, 1884–1887 (1998)

18. Ma, J., Tang, J., Zhang, A.H., Jia, Y.: Robustness and breakup of the spiral wave in a two-dimensional lattice network of neurons. Sci. China Ser. G **53**, 672–679 (2010)
19. Ma, J., Wu, Y., Ying, H.P., Jia, Y.: Channel noise-induced phase transition of spiral wave in networks of Hodgkin–Huxley neurons. Chin. Sci. Bull. **56**, 151–157 (2011)
20. Wang, C.N., Ma, J., Liu, Y., Huang, L.: Chaos control, spiral wave formation, and the emergence of spatiotemporal chaos in networked Chua circuits. Nonlinear Dyn. **67**, 139–146 (2012)
21. Ma, J., Huang, L., Tang, J., Ying, H.P., Jin, W.Y.: Spiral wave death, breakup induced by ion channel poisoning on regular Hodgkin–Huxley neuronal networks. Commun. Nonlinear Sci. Numer. Simul. **17**, 4281–4293 (2012)
22. Fox, R.F., Lu, Y.: Emergent collective behavior in large numbers of globally coupled independently stochastic ion channels. Phys. Rev. E **49**, 3421 (1994)
23. Schmid, G., Goychuk, I., Hänggi, P.: Stochastic resonance as a collective property of ion channel assemblies. Europhys. Lett. **56**, 22 (2001)
24. Jung, P., Shuai, J.: Optimal sizes of ion channel clusters. Europhys. Lett. **56**, 29 (2001)